

Control of Supercavitating Vehicles Based on Robust Pole Allocation Methodology

Ziyao Cao

College of Marine Engineering, Northwestern Polytechnical University

Xi'an, Shaanxi Province, China

E-mail: caoziyao@nwpu.edu.cn

Received: December 27, 2010

Accepted: January 7, 2011

doi:10.5539/mas.v5n2p204

Abstract

Supercavitating vehicles can achieve very high speed but the hydrodynamic forces and the forces balance of which are different from common underwater vehicles, because the most surfaces of the vehicle are in cavity. Compared to a fully-wetted vehicle for which substantial lift is generated due to vortex shedding off the hull, a supercavitating vehicle is enveloped by gas cavity and thus the lift is provided by control surface deflections of the cavitator and fins, as well as planing force between the vehicle and the cavity. In this paper, a proper dynamic model of the vehicle for pitch was presented by analyzing and studying hydrodynamic forces on the vehicle. Then robust pole allocation methodology was used to design the controller, and it got good dynamic stability. It provided a necessary theoretical dependence for farther studying the dynamic control problem of supercavitating vehicles.

Keywords: Hydrodynamic force, Dynamic modeling, Robust pole allocation algorithm, Supercavitating vehicle

1. Introduction

Because the supercavitating vehicle's surfaces are enveloped by cavity entirely or mostly, there is only a small portion of the body contacting with water. The vehicle has very small skin friction drag, this allows it to obtain high speed underwater---more than 100m/s. But it is really hard to model, control and maneuver a supercavitating vehicle. The controlling, guidance and stability are achieved only by the small region in the head and aft of the body.

There is a cavitator at the head of the vehicle which could generate cavity and provide some amount of lift. Fins are in the aft of the body and could penetrate through the cavity to provide tail lift(Wei.Cao,Jingjie.Wei, Cong Wang et.al, 2006). The vehicle loses most buoyancy of the fluid when it is in cavity, there are some ways to balance body' weight: the planning force at the tail and the cavitator lift force provide lift together(Yu.N.Savchenko, 2001), and when the vehicle travel stability the body does not contact with the cavity wall, fins help the cavitator to provide some amount of lift to support the weight of the vehicle(ANUKUL GOEL, 2005). In the second case, cavitator and the fins could be control surfaces to control the vehicle. There is not much paper in this field recently. In (ANUKUL GOEL, 2005), it studied the robust control of supercavitating vehicle. Savchenko studied the problem of controlling of the supercavity vehicles(Savchenko Yu N, 2001). In (R.Rand,R.Pratap,D. amani,J.Cipolla, I.Kirschner, 2002), it studied the impact dynamics of a supercavitating underwater projectile. S.S.Kulkarni and R.Pratap studied on the dynamics of a supercavitating projectile(S.S.Kulkarni and R.Pratap, 2000). In (Huiping Fu,Chuanjing lu,Lei Wu, 2004), it explored six degree-of-freedom fin forces for the supercavitating test bed vehicle.

Studying on this field is just at the beginning in our country, the published paper was mostly concerning on the study of the drag characteristics and the shape of the supercavity vehicles, such as in (Xulong Yuan,Yuwen Zhang,Lehua Liu et.al, 2004)(Xin Chen,Chuanjing Lu,Lei Wu, 2005)(Yuan zihuai, Qian xingfang, 2001)(Kirschner I N.Fine Neal E,Uhlman James S,Kring David C, 2002)(Logvinovich G.V, 2001). In this paper, the dynamic model was built when the body was traveling stably, which took no account of the contraction between the body and the cavity wall. Fins provided some amount of lift.

In this paper, a simple nonlinear model of supercavitating vehicle in longitude plane was built, and linear equations and state space model of longitude motion were obtained by using small disturbance theory. The simulation results were agreement with the experiment observation. The system was unstable but completely controllable, so robust pole allocation was used to control the body, the simulation curves show that robust pole

allocation algorithm was simple and effective, and they were agreement with hydrokinetics theory analysis.

2. Equations of Motion

2.1 Define the Reference Frame

As the motion of the vehicle in cavity is same as aircraft in air, a reference frame usually used in flight mechanics is used to describe the motion of the vehicle. Earth-fixed reference $Exyz$ is defined firstly to describe the motion of gravity center of the vehicle. It is centered at any conveniently chosen point. Ez axis pointed in downward direction, i.e., the direction of the gravity. Ex axis and Ey axis were in the horizon plane and were perpendicular to each other. A body-fixed frame $Ox_b y_b z_b$ is defined to describe rotation of body: the origin is the center of gravity of the body, Ox_b axis is symmetry axis, pointed the head of the vehicle, $x_b Oz_b$ is the symmetric section of the vehicle, Oz_b axis pointed downward.

A velocity coordinate $Oxyz$ is defined to describe the relative location between velocity vector of the centre of gravity and the vehicle and to confirm the forces acted on the body. The three axes were same as the common underwater vehicles. Attack angle α and sideslip angle β were same as common underwater vehicle.

2.2 Forces on Vehicle

When the vehicle is traveling stably, a large portion of its surfaces were in cavity, only cavitator and fins were in water. Thus the motion is determined by the hydrodynamics forces and moments produced by cavitator and fins, when vehicle is pitch in longitude plane.

2.2.1 Forces on Cavitator

The cavitator discussed in this paper only had one degree: it could rotate about the axis which paralleled Oy_b , which is defined as δ_c . Because the cavitator dimension is very small compared to the whole body, it is assumed that the rotation center is the position of cavitator in body-fixed frame.

The forces acting on the cavitator were lift and drag produced by hydrodynamic forces. The lift is along Oy axis and the drag is along $-Ox$ axis. cl_c is coefficient of lift and cd_c is coefficient of drag. Reference (Yuriy D.Vlasenko, 2003) provided formulas to compute them for flat disk cavitator.

$$\begin{aligned} cd_c &= 0.82(1 + \sigma) \cdot \cos^2(\alpha_c + \delta_c) \\ cl_c &= 0.82(1 + \sigma) \cdot \cos(\alpha_c + \delta_c) \cdot \sin(\alpha_c + \delta_c) \end{aligned} \quad (1)$$

The lift L_c and drag D_c on the cavitator were:

$$L_c = \frac{1}{2} \rho V_c^2 S_c cl_c, \quad D_c = \frac{1}{2} \rho V_c^2 S_c cd_c \quad (2)$$

Where, V_c is the cavitator's velocity, it is equal to vehicle's velocity. S_c is the transom section of the cavitator, ρ is density of water, σ is cavitation number. δ_c is rotation angle of the cavitator, α_c is attack angle of the cavitator. When cavitator had deflection δ_c , lift on cavitator, in body frame, can be calculated in Equation (3).

$$F_{c,z_b} = -L_c \cos(\delta_c - \alpha_c) - D_c \sin(\alpha_c - \delta_c) \quad (3)$$

2.2.2 Forces on fins

1.2.2.1 Calculation of Cavity Shape

It is necessary to know the cavity shape when discussed the forces on fins. In this paper, it is assumed that the cavity is symmetry. Excursion of cavity centerline produced by gravity is neglected, and the impact between the vehicle and cavity wall caused by cavity section's transform motion is neglected too. Reference [13] gave the empirical formulas for the undisturbed cavity based on theory of independent expansion and a large amount experimental data.

$$\begin{aligned} R(x) &= R_n \left(1 + \frac{3x}{R_n} \right)^{\frac{1}{3}}, & x \leq x_1 \\ R(x) &= R_c \sqrt{1 - \left(1 - \frac{R_1^2}{R_c^2} \right) \left(1 - 2 \frac{x - x_1}{L_{cav} - 2x_1} \right)^2}, & x \geq x_1 \end{aligned} \quad (4)$$

Where $R(x)$ is current radius of the cavity. R_n is cavitated radius. x is the distance from the cavitator. $x_1 \approx 2R_n$, R_c is cavity middle section radius, L_{cav} is the length of cavity. They could be written as the function of cavitation number σ [13].

$$R_c = \sqrt{3.659 + \frac{0.761}{\sigma}}, L_{cav} = 4 + \frac{3.595}{\sigma} \quad (5)$$

From (5), the cavity radius in the location of fins could be calculated, thus the immersion areas of fins and the amount and direction of fin lift could be obtained.

1.2.2.2 Forces on Fins

Fins were in the aft portion of the vehicle, whose directions were along Oy , whose deflections were defined by δ_f . The forces can be written as in (6).

$$L_f = \frac{1}{2} \rho V^2 S c l_f, \quad D_f = \frac{1}{2} \rho V^2 S c d_f \quad (6)$$

Where, L_f is lift acting on the fins, D_f is drag acting on the fins. ρ is the density of water, V is the velocity of fins in earth-fixed frame. S were the immersion areas of the fins. $c l_f$ And $c d_f$ were coefficient of lift and coefficient of drag of fins respectively. $c l_f$ and $c d_f$ could be calculated in (7) and (8).

$$c l_f = 0.82(1 + \sigma) \cos(\alpha_f + \delta_f) \sin(\alpha_f + \delta_f) \quad (7)$$

$$c d_f = 0.82(1 + \sigma) \cos^2(\alpha_f + \delta_f) \quad (8)$$

Where α_f, δ_f is attract angle and deflection angle of fins respectively. Similarity, the lift on fins, in body frame, can be calculated as in (9).

$$F_{f,z_b} = L_f \cos(\delta_f - \alpha_f) - D_f \sin(\delta_f - \alpha_f) \quad (9)$$

2.3 Moments Equation

Because the origin of body-fixed frame is at center of gravitation of the vehicle, the moments of gravitational forces were zero. There were only two lift moments produced by cavitator and fins respectively for pitch.

2.3.1 Moments Produced by Cavitator

Cavitator is located at the head of the vehicle, and the lift acted on the geometry center of the cavitator. It is assumed that the geometry centre of the cavitator had no deflection along Ox_b , thus its coordinate of the geometry centre of the cavitator is $(X_c, 0, 0)$ in body-fixed frame. Thus the moment of lift acting on cavitator about center of gravitation of the vehicle can be written as in formula (10).

$$M_{c,z_b} = X_c [D_c \sin(\alpha_c - \delta_c) + L_c \cos(\delta_c - \alpha_c)] \quad (10)$$

2.3.2 Moments Produced by Fins

Similarly, moments of lift acting on fins about center of gravitation of the vehicle can be written as in (11).

$$M_{f,y_b} = -X_f L_f \cos(\delta_f - \alpha_f) + X_f D_f \sin(\delta_f - \alpha_f) \quad (11)$$

Where X_f is coordinate of fins in body-fixed frame.

3. Dynamic Equations of Motion

It is assumed that the vehicle is a rigid body and its mass is constant. Additional mass produced by body rotation is neglected. Thus from (3) and (9), and using Newton law, the dynamic equations can be derived in (12).

$$\begin{aligned} m(\dot{w} + pv - uq - g \cos \theta)_b = \\ -L_c \cos(\delta_c - \alpha_c) - D_c \sin(\alpha_c - \delta_c) \\ L_f \cos(\delta_f - \alpha_f) - D_f \sin(\delta_f - \alpha_f) \end{aligned} \quad (12)$$

Where p is rotation angle rate around Ox_b axis. q is rotation angle rate around Oy_b axis. u is velocity component along Ox_b , v is velocity component along Oy_b , w is velocity component along Oz_b . \dot{w} is

acceleration of w .

Because Ox_b, y_b is in the symmetry section of the vehicle, inertia product $J_{x_b z_b} = 0$ and $J_{z_b y_b} = 0$. When Ox_b is superposition with the inertia axis, inertia product $J_{x_b y_b} = 0$. Using Newton law of rotation, thus the rotation equation (13) is obtained.

$$\begin{aligned} I_y \dot{q} + \eta p (I_x - I_z) &= X_c [D_c \sin(\alpha_c - \delta_c) + L_c \cos(\delta_c - \alpha_c)] \\ -X_f L_f \cos(\delta_f - \alpha_f) + X_f D_f \sin(\delta_f - \alpha_f) & \end{aligned} \quad (13)$$

4. Control equations

4.1 Linearization

Took straight level flight as the benchmark of the vehicle, u_0 is the velocity of the vehicle, θ_0 is pitch angle of the vehicle. They were undisturbed parameters, u_0 is obtained by mathematical method. Δ is small disturbance of state variable. Substituted Δ into the equation of motion and neglected the second or more than second order at benchmark condition, then subtracted benchmark equation of motion, thus small disturbance equation of linearization can be derived.

Undisturbed parameters were substituted into equation (12) to obtain equation (14).

$$-mg \cos \theta_0 = F_0 \quad (14)$$

Δ can be substituted into equation (12) to obtain disturbance equation (15).

$$\begin{aligned} m \cdot \frac{d}{dt} (w_0 + \Delta w) + m \cdot (p_0 + \Delta p) (v_0 + \Delta v) \\ - m \cdot (u_0 + \Delta u) (q_0 + \Delta q) - m \cdot g \cos(\theta_0 + \Delta \theta) = F_0 + \Delta F \end{aligned} \quad (15)$$

Subtracted equation (14) from equation (15).

$$m(\Delta \dot{w} - u_0 \Delta q + g \Delta \theta \sin \theta_0) = \Delta F \quad (16)$$

The moments linearization equation can be obtained in analogous to (16).

$$I_y \Delta \dot{q} = \Delta M \quad (17)$$

3.2 Control Differential Equations

Only the pitch of the vehicle is discussed in this paper. δ_c and δ_f were chosen as control variable, w and q were state variable. Thus (18) and (19) were obtained.

$$\Delta F = \left(\frac{\partial F}{\partial w} \right)_0 \Delta w + \left(\frac{\partial F}{\partial q} \right)_0 \Delta q + \left(\frac{\partial F}{\partial \delta_c} \right)_0 \Delta \delta_c + \left(\frac{\partial F}{\partial \delta_f} \right)_0 \Delta \delta_f \quad (18)$$

$$\Delta M = \left(\frac{\partial M}{\partial w} \right)_0 \Delta w + \left(\frac{\partial M}{\partial q} \right)_0 \Delta q + \left(\frac{\partial M}{\partial \delta_c} \right)_0 \Delta \delta_c + \left(\frac{\partial M}{\partial \delta_f} \right)_0 \Delta \delta_f \quad (19)$$

Where, the subscript denoted differential of the benchmark state of the vehicle. $\left(\frac{\partial f}{\partial w} \right)_0$ can be expanded as (20).

$$\left(\frac{\partial f}{\partial w} \right)_0 = \frac{\partial}{\partial w} (f_{c,z} + f_{f,z}) \quad (20)$$

Where $f_{c,z}$ is the lift acting on cavitator in body-fixed frame, $f_{f,z}$ is the lift acting on fins in body-fixed frame.

Equation (3) and (9) can be substituted into (20), and then calculated the derivation of it at respect to w . Equation (21) can be derived.

$$\begin{aligned} \frac{\partial f}{\partial w} &= -\frac{\partial D_c}{\partial w} \sin(\alpha_c - \delta_c) - \frac{\partial L_c}{\partial w} \cos(\delta_c - \alpha_c) - D_c \cos(\alpha_c - \delta_c) \frac{\partial \alpha_c}{\partial w} + L_c \sin(\delta_c - \alpha_c) \frac{\partial \alpha_c}{\partial w} \\ &- \frac{\partial D_f}{\partial w} \sin(\delta_f - \alpha_f) + \frac{\partial L_f}{\partial w} \cos(\delta_f - \alpha_f) + D_f \cos(\delta_f - \alpha_f) \frac{\partial \alpha_f}{\partial w} + L_f \sin(\delta_f - \alpha_f) \frac{\partial \alpha_f}{\partial w} \end{aligned} \quad (21)$$

Where, $\frac{\partial \alpha_c}{\partial w}, \frac{\partial L_c}{\partial w}, \frac{\partial D_c}{\partial w}, \frac{\partial \alpha_f}{\partial w}, \frac{\partial L_f}{\partial w}, \frac{\partial D_f}{\partial w}$ were needed to be calculated. From the definition of attack angle and sideslip angle, Equation (22), (23) and (24) can be derived.

$$\tan(\alpha_c) = \frac{w_c}{u_c}. \quad (22)$$

$$\tan(\beta_c) = \frac{-v_c}{V_c}. \quad (23)$$

$$V_c^2 = v_c^2 + u_c^2 + w_c^2. \quad (24)$$

According to the relationship between the deflection of the cavitator and the body-fixed frame, the velocity component of the cavitator u_c, v_c, w_c can be written as formula (25), (26) and (27).

$$u_c = \cos \delta_c (u + qz_c - ry_c) - \sin \delta_c (w + py_c - qx_c) \quad (25)$$

$$v_c = v + pz_c - rx_c \quad (26)$$

$$w_c = \sin \delta_c (u + qz_c - ry_c) + \cos \delta_c (w + py_c - qx_c) \quad (27)$$

Where, x_c, y_c and z_c were coordinate components of the geometry of the cavitator respectively. p, q and r were rotation angles rate of the center of gravitation of the vehicle around Ox_b axis, Oy_b axis and Oz_b axis respectively. The variation of (25), (26) and (27) with respect to w can be obtained at reference flight condition.

$$\frac{\partial u_c}{\partial w} = -\sin \delta_c \quad (28)$$

$$\frac{\partial v_c}{\partial w} = 0 \quad (29)$$

$$\frac{\partial w_c}{\partial w} = \cos \delta_c \quad (30)$$

As, $\frac{\partial \alpha_c}{\partial w} = \frac{\partial \alpha_c}{\partial w_c} \frac{\partial w_c}{\partial w}$, calculating variation of (22) with respect to w can derive $\frac{\partial \alpha_c}{\partial w_c}$. Substituted (30) into

$\frac{\partial \alpha_c}{\partial w} = \frac{\partial \alpha_c}{\partial w_c} \frac{\partial w_c}{\partial w}$, thus derived $\frac{\partial \alpha_c}{\partial w} = \frac{1}{u_0}$. Then $\frac{\partial L_c}{\partial w}, \frac{\partial D_c}{\partial w}$ were needed to be calculated.

$$\frac{\partial L_c}{\partial w} = \frac{1}{2} \rho S_c \left[2V_c c l_c \frac{\partial V_c}{\partial w} + V_c^2 \frac{\partial c l_c}{\partial w} \right] \quad (31)$$

Where $\frac{\partial \alpha_c}{\partial w} = \frac{1}{u_0}, \frac{\partial V_c}{\partial w} = 0, \frac{\partial c l_c}{\partial w}$ and $\frac{\partial c d_c}{\partial w}$ can be calculated from (1). Finally

$\frac{\partial \alpha_f}{\partial w}, \frac{\partial L_f}{\partial w}, \frac{\partial D_f}{\partial w}$ can be obtained analogically.

Only w, q changed at reference flight in pitch plane, thus $\Delta \theta = 0$. Then the state space expression can be written as (32).

$$\begin{bmatrix} \Delta \dot{w} \\ \Delta \dot{q} \end{bmatrix} = \begin{bmatrix} \frac{1}{m} \left(\frac{\partial f}{\partial w} \right)_0 & \frac{1}{m} \left(\frac{\partial f}{\partial q} \right)_0 + u_0 \\ \frac{1}{I_y} \left(\frac{\partial M}{\partial w} \right)_0 & \frac{1}{I_y} \left(\frac{\partial M}{\partial q} \right)_0 \end{bmatrix} \begin{bmatrix} \Delta w \\ \Delta q \end{bmatrix} + \begin{bmatrix} \frac{1}{m} \left(\frac{\partial f}{\partial \delta_c} \right)_0 & \frac{1}{m} \left(\frac{\partial f}{\partial \delta_f} \right)_0 \\ \frac{1}{I_y} \left(\frac{\partial M}{\partial \delta_c} \right)_0 & \frac{1}{I_y} \left(\frac{\partial M}{\partial \delta_f} \right)_0 \end{bmatrix} \begin{bmatrix} \delta_c \\ \delta_f \end{bmatrix} \quad (32)$$

4. Controller design based on robust pole allocation

A vehicle model is parameterized in generic terms of body radius, body length, and body density relative to the surrounding fluid. The fore body shape is assumed to be a right cylindrical cone and the aft two-thirds is

assumed to be cylindrical. The cavitator is a flat disk.

The model parameters for numerical examples were(John dzielski,Andrew kurdila, 2003): cavitator radius $R_n = 0.0191\text{m}$, the radius of the vehicle $R = 0.05808\text{m}$, cavitation number $\sigma = 0.02$, stable velocity $u_0 = 124\text{ m/s}$, body length is 1.80m , the distance between fins and cavitator is 1.2m . Substituting these parameters into (32), the state space equations of the vehicle can be derived.

$$A = \begin{bmatrix} -20.0072 & 145.866 \\ 248.057 & -271.07 \end{bmatrix}, \quad (33)$$

$$B = \begin{bmatrix} 1240.45 & -638.177 \\ 15379.5 & -775.382 \end{bmatrix} \quad (34)$$

$$C = \begin{bmatrix} 1 & 0 \\ 0 & 1 \end{bmatrix} \quad (35)$$

$$D = 0 \quad (36)$$

Analyzing matrix A and B, we knew that the system is unstable. The output is divergence and changed sharply. It is shown in Fig. 1.

It can be seen that when $\delta_f = 1^\circ, \delta_c = 1^\circ$, w and q responded between 0s to 1.2s. The response curves rose sharply. The largest value could be reach 10^{30} . Clearly, the system is very unstable, which is agreement with the experiment phenomenon.

As the system is unstable, a control method should be used to control the system. For the system is completely controllable, robust pole allocation method is used to locate the poles of the system arbitrarily. Here, we specified the location of the poles based on the criterion of the system close loop response. The state feedback matrices were:

$$k = \begin{bmatrix} -1.0181 & -0.1977 \\ -11.5640 & -11.4865 \end{bmatrix} \quad (37)$$

Performance of the system is improved prominently after pole allocation. The step response of system after pole allocation is shown in Fig.2.

From Fig.2, it can be seen that the dynamic response curves were smoothness and satisfied basis performance criteria. The dynamic stability is better. Simultaneity noted that w, q were sensitiver to δ_c step command than to δ_f , it is provided that δ_c has better control effect than δ_f , which is agreement with hydrokinetics analysis.

5. Conclusions

The reference frame usually used in designing aircraft in Anglo-American country is used to analyze hydrodynamic forces on supercavitating vehicle in this paper. Then a simple control model was built. It was seen that the system is unstable but completely controllable by studying and analyzing the state space expression. So robust pole allocation method was presented to design state feedback controller for the system. The simulation results denoted that the method could resolve the unstable problem of the system and achieve better dynamic performance.

When the attack angle changed, the planning forces are produced by the reaction between tail of the vehicle and cavity wall. But in the former work, the planning forces were not included in the model, which were primary lifts in the aft portion of the body at special times. So it is needed to be studied and discussed in future work.

References

- ANUKUL GOEL. (2005). Robust control of supercavitating vehicles in the presence of dynamic and uncertain cavity[D]. Florida:University of Florida.
- Huiping Fu,Chuanjing lu,Lei Wu. (2004). Numerical Research on drag Reduction Charateristics of Supercavitating Body of Revolution, *Journal of Ship Mechanics*, vol. 20, no. 1, pp. 84-91.
- John dzielski,Andrew kurdila. (2003). A benchmark control problem for s upercavitating vehicles and an initial investigation of solutions. *Journal of Vibration and control*.vol.9,no.pp.791-804.
- Kirschner I N.Fine Neal E,Uhlman James S,Kring David C. (2002). Numerical modeling of supercavitating flows. *Lecture Series on Supercavitating flows*, RTO Lecture Series 005.

Logvinovich G.V. (2001). Hydrodynamics of flows with free boundaries, *Kiev,Naukova dumka Publ.House*,208p. 1069.

R.Rand,R.Pratap,D. amani,J.Cipolla, I.Kirschner. (2002). Impact dynamics of a supercavitating underwater projectile. *Proceedings of the Third International Symposium on Performance Enhancement for Marine Applications*, Newport, I, pp. 215-223, 197.

S.S.Kulkarni and R.Pratap. (2000). Studies on dynamics of a supercavitating projectile, *Applied Mathematical Modeling*, vol. 24, pp. 113-129.

Savchenko Yu N. (2001). Control of Supercavitating Motion of Bodies. *VKI Special Course on Supercavitating Flows*, Brussels: RTO-AVT and VKI, RTO-EN-010(11).

Wei.Cao,Jingjie.Wei, Cong Wang et.al. (2006). Current status problems and applications of supercavitation technology, *Advances in mechanics*, vol.36, no. 4, pp.571-579.

Xin Chen,Chuanjing Lu,Lei Wu. (2005). The investigation on morphology of ventilated supercavity. *Journal of Ballistics*, vol. 17, no. 1, pp. 1-8.

Xulong Yuan,Yuwen Zhang,Lehua Liu et.al. (2004). Experimental investigation of ventilated supercavity on underwater vehicle model, *Chinese Journal of Applied Mechanics*, vol. 21, no. 3, pp. 33-39.

Yu.N.Savchenko. (2001). Control of supercavitation flow and stability of supercavitating motion of bodies. *In: Van den Braembussche,ed.VKI Special Course on Supercavitating Flows*,Brussels,2001-02-12~116.Brussels:RTO-AVT and KVI, RTO-EN-010(11).

Yuan zihuai, Qian xingfang. (2001). Control flight mechanics and computer simulation. *Eds.Beijing: Publishing House of National Defence Industry*, pp.5-25.

Yuriy D.Vlasenko. (2003). Experimental investigation of supercavitation flow regimes at subsonic and transonic speeds. *Fifth international symposium on cavitation(cav2003)*. Japan, Osaka.

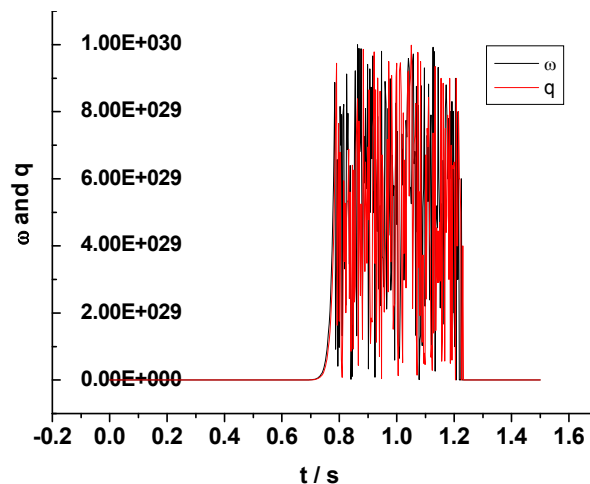


Figure 1. $\delta_f = 1, \delta_c = 1$, response of w and q

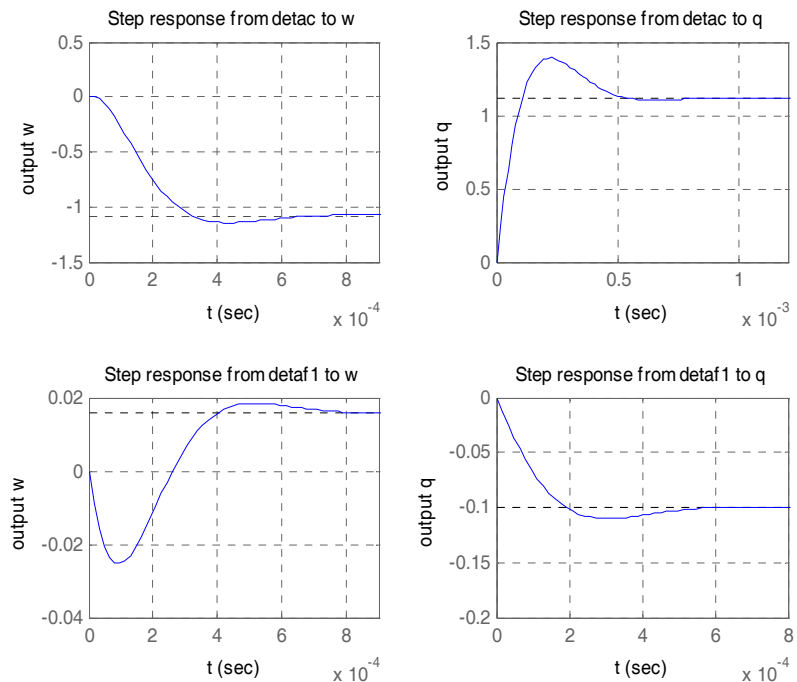


Figure 2. System step response